June 2008 *Volume 2 Issue 1*

Trade Science Inc.

Nano Science and Nano Technology
An Indian Journal

Full Paper

NSNTAIJ, 2(1), 2008 [01-07]

Co_3O_4 and CuO nanoparticles obtained by a solvent-free method

A.Vazquez-Olmos*[1], A.L.Ramos-Bautista[1], A.L.Fernandez-Osorio[2], R.Sato-Berru[1]
[1]Centro de Ciencias Aplicadas y Desarrollo Tecnologico, (MEXICO)
[2]Facultad de Estudios Superiores, Cuautitlan-1, Universidad Nacional Autonoma de México, Coyoacan, Mexico D. F., 04510, (MEXICO)
Phone: (52-55) 5622 8616 ext. 1154; Fax: (52-55) 5622 8651
E-mail: america.vazquez@aleph.cinstrum.unam.mx
Received: 7th March, 2008 ; Accepted: 12th March, 2008

ABSTRACT

Co_3O_4 and CuO nanoparticles have been successfully synthesized *via* an uncomplicated mechanochemical solvent-free method. Their crystalline structures and their average diameters between 5 and 8 nm, were determined from XRD patterns and by HR-TEM images. Particle sizes were controlled through the concentration of starting materials and heating temperature. The UV-visible electronic absorption, raman spectroscopy and electronic paramagnetic resonance spectra of Co_3O_4 and CuO nanocrystals show clear evidence of the quantum size effect. The mechanochemical method as a simple process provides economically viable route for large-scale nanomaterials production.

KEYWORDS

Mechanochemical reaction;
Nanoparticles;
Transition metal oxides.

INTRODUCTION

Transition metal oxides represent one of the most diverse types of materials with important structure-related properties. Many of them exhibit conductivity, superconductivity, ferroelectricity, magnetism, magneto resistivity, or gas-sensing capabilities[1-8]. It is evident that the synthesis of metal oxide nanostructures will lead to important developments in the construction of new devices. This paper is devoted to the production of Co_3O_4 and CuO nanoparticles. Cobalt oxide Co_3O_4 is a p-type semiconductor with a narrow band gap of 1.6 eV[9]. This compound is a mixed-valence oxide $[Co(II)Co(III)_2O_4]$ with a normal spinel crystal structure based on an array of cubic close-packed oxide ions, in which Co(II) ions occupy the tetrahedral 8a sites and Co(III) ions occupy the octahedral 16d sites [10-11]. It is known that Co_3O_4 bulk crystal exhibits antiferromagnetism, with a Neel temperature (T_N) of 33 K[12]. This cobalt oxide has a wide range of industry applications including anode materials for rechargeable Li-ion battery, catalysts, pigments, gas sensors, magnetic materials and as intercalation compounds for energy storage[13-16]. These applications are related to particle size and surface effects.

Copper oxide CuO presents certain interest, because it is a p-type semiconductor with a narrow band gap between 1.21 and 1.5 eV[17,18], it has three magnetic phases: antiferromagnetic phase below Néel temperature ($T_N \approx 230$ K), a fluid like phase between the Néel temperature and 630 K, and above the Néel temperature, where paramagnetic ordering is observed[19].

Full Paper

Distinct of MnO, FeO, CoO and NiO which crystallize in the NaCl structure, CuO is unique in having a monoclinic unit cell and square-planar coordination of copper by oxygen[1]. The effect of the electronic configuration of Cu(II) on electronic and phononic characteristics of mixed oxides, CuO has made a fundamental compound of several high-Tc superconductors[20-21]. In addition, it forms the basis of technologically important materials is used in heterogeneous catalysts, gas sensors, optical switch, magnetic storage media, lithium batteries and solar-energy transformation[22-25].

In the past decades, different techniques have been employed in order to prepare nanocrystalline oxides with controlled size and shape, such as thermal decomposition of metallic salts under an oxidizing atmosphere, sol-gel method, colloidal method, hydrothermal processing, reduction/oxidation, homogeneous precipitation, metal organic chemical vapor deposition (MOCVD) and mechanochemical processing[26-36].

Look for the future development and the applications of metal oxide nanoparticles, it is very important to employ inexpensive synthesis methods that produce adequate amounts under mild reaction conditions.

Mecanochemically initiated solid-state processes have recently become a subject of intense investigations, due to the potential applications of such reactions in technology, in particular, for the development of the so called dry processes, which are more environmentally friendly and cost efficient than the current adopted technologies[37-40]. Furthermore, this method yields the respective product as a highly dispersed phase, which can be useful for the subsequent technological steps.

Mechanochemical route involves the mechanical activation of solid state displacement chemical reactions, either during milling (using ball or planetary mill or well an agate mortar) or during following heat treatment. This procedure is particularly suitable for large-scale production due to its simple process and low cost[41].

Nowadays, the synthesis of nanocrystalline materials based on mechanochemical method is a quickly expanding field of solid state science, covering a variety of subjects such as alloys, nanostructured materials, amorphous and disordered solids, metastable materials, nanomagnetics, etc.

Recently, a wide variety of nanosized oxides have been synthesized by mechanochemical route including Co_3O_4 and CuO, however the reported average crystal size oscillates between 12 and 50 nm, employing milling times until 60 hrs and in some cases a thermal treatment of the precursors between 300 and 700^{0}C was necessary to carry out[31,35,36].

Here we present the synthesis of Co_3O_4 and CuO nanoparticles with average diameters between 5 and 8 nm, by an easy and reproducible solvent-free solid-solid synthesis method, starting from their respective chloride or acetate salts in the presence of sodium hydroxide. Co_3O_4 Nps were obtaining after heating at 150 by 30 min the $Co(OH)_2$ prepared by mechanochemical activation in an agate mortar, at room temperature. In contrast, CuO Nps were easily synthesized at room temperature. Spectroscopic and structural studies on these nanoparticles were carried out. The procedure followed in this work constitutes an important advance in the preparation of nanostructured metallic oxides, specially, for applications that require clean nanostructured materials.

EXPERIMENTAL

Materials

Cobalt acetate tetrahydrate, $Co(OAc)_2 4H_2O$ (98% Aldrich), cobalt chloride hexahydrate, $CoCl_2 \cdot 6H_2O$ (98% Aldrich), copper acetate monohydrate, $Cu(OAc)_2 \cdot H_2O$ (98% Aldrich), copper chloride dihydrate, $CuCl_2 \cdot 2H_2O$ (98% Aldrich), sodium hydroxide NaOH (98% Aldrich) and acetone $CO(CH_3)_2$ (Aldrich 99.5%) were purchased and used as received, without further purification. Ultra pure water (18 MΩcm^{-1}) was obtained from a Barnstead E-pure deionization system.

Synthesis

Co_3O_4 nanoparticles were obtained in two steps. In the first 5×10^{-3} moles (1.2454g) of $Co(OAc)_2 \cdot 4H_2O$ (sample A) or 5×10^{-3} moles (1.1896g) of $CoCl_2 \cdot 6H_2O$ (sample B), were mixed and milled with 0.4g of NaOH in an agate mortar at room temperature, until the color of the powder kept unchanged, about 30 minutes. In both cases, after this time a dark green powder of $Co(OH)_2$ was obtained (reaction a). This compound was washed 4 times with water and 2 times with acetone, and then was air dried. In the second step, the cobalt hydroxide was heated at 150°C for 30 minutes;

subsequently, a black powder of Co_3O_4 nanoparticles was obtained (reaction b).

$$\text{(a)}\quad CoX_2 + 2\,NaOH \xrightarrow[\text{milling}]{R\,T} Co(OH)_2 + 2\,NaX$$

$$X = Cl^- \text{ or } CH_3COO^-$$

$$\text{(b)}\quad Co(OH)_2 + 1/2\,O_2 \xrightarrow[30\ min]{150^0C} Co_3O_4 + 3H_2O$$

On the other hand CuO nanoparticles were obtained from 5×10^{-3} moles (0.9982g) of $Cu(OAc)_2\cdot H_2O$ (sample C) or 5×10^{-3} moles (0.8524g) of $CuCl_2\cdot 2H_2O$ (sample D), mixed and milled with 0.4g of NaOH in an agate mortar at room temperature, until the color of the powder kept unchanged, about 20 minutes. Then, a dark brown powder of CuO nanoparticles was obtained (reaction c). The powder was washed and dried following the procedure previously described

$$\text{(c)}\quad CuX_2 + 2\,NaOH \xrightarrow[\text{milling}]{R\,T} CuO + 2\,NaX + H_2O$$

$$X = Cl^- \text{ or } CH_3COO^-$$

Instruments

The UV-visible electronic absorption spectra of the powdered samples were obtained by diffuse reflectance technique, with an Ocean Optics USB2000 miniature fiber optic spectrometer. The Raman spectra, from 100 to 900cm^{-1}, were evaluated using a Nicolet Almega XR dispersive raman spectrometer and detected by a CCD camera, at 25 seconds and a resolution of~4cm^{-1}. The excitation beam was a Nd:YVO_4 532 nm laser and the incident power on the sample was ~3 mW. The X-ray diffraction patterns were performed at room temperature with Cu Kα radiation (λ = 1.5406Å) in a D5000 Siemens diffractometer; diffraction intensity was measured between 2.5° and 70°, with 2θ step of 0.02° for 0.8s per point. High-resolution transmission electron micrographs (HR-TEM) were obtained in a JEOL 2010 FasTEM analytical microscope, operating at 200 kV, by deposition of a drop of the powdered transition metal oxide dispersed in N,N′-dimethylformamide (DMF) onto 300 mesh Cu grids coated with a carbon layer. X-band electronic paramagnetic resonance (EPR) data were obtained on a Brücker ELEXSYS spectrometer, with a center field of 4080 G, modulation of amplitude of 0.2, time constant of 0.025 s, scan time of 2 min, and microwave power of 20 mW.

RESULTS AND DISCUSSION

$Co(OH)_2$ and Co_3O_4 Nps X-ray diffraction patterns are shown in figure 1a-c. All diffraction peaks can be perfectly indexed to the cobalt hydroxide (JCPDS card 74-1058) and the cubic phase of Co_3O_4 spinel structure (JCPDS card 73-1701), with a unit symmetry described by the space group Fd3m and lattice parameter a = 8.083Å (figures 1b and 1c). The diffraction peaks are markedly broadened, which is indicative of a fine crystallite size. In all cases, no peaks of impurity are observed in the XRD patterns.

In order to determine the Co_3O_4 Nps average size, the peak broadening method using the classical Scherrer equation over the (220) and (400) reflections was employed. Co_3O_4 Nps obtained from cobalt acetate (sample A) have an average size of 5.0 ± 0.28 nm (fig-

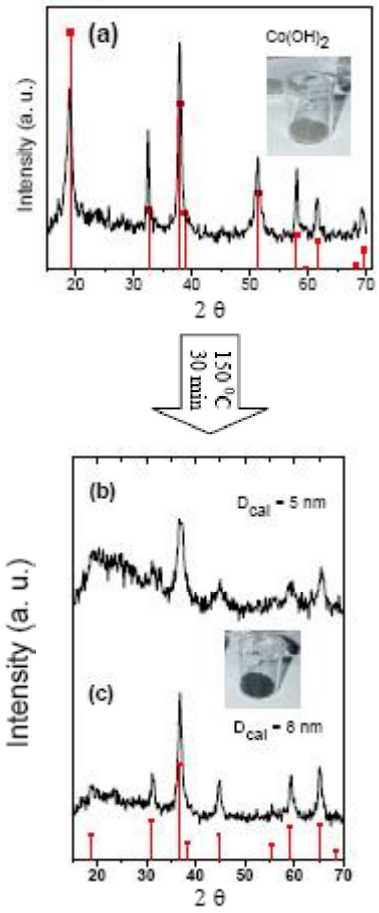

Figure 1: XRD patterns of (a) $Co(OH)_2$ obtained at room temperature after milling in an agate mortar, (b) Co_3O_4 Nps obtained from the cobalt acetate salt (sample A), and (c) Co_3O_4 Nps obtained from cobalt chloride salt (sample B)

Full Paper

ure 1b), while those obtained from cobalt chloride (sample B) have an average size of 8 ± 0.21 nm(figure 1c).

In the following discussion we will refer to Co_3O_4 Nps in a general form because the UV-Visible absorption and Raman spectra for samples A and B are very similar.

With the aim of to study the optical response of the Co_3O_4 Nps, UV-Visible electronic absorption spectroscopy using diffuse reflectance technique (DRS) was obtained. Figure 2 shows the Co_3O_4 bulk and Nps absorption spectra. In both, two wide absorption bands appear; the first, with a maximum at 352 nm for the bulk and the Nps, involves charge transfer transitions from $O^{2-} \rightarrow Co^{2+}$ and $O^{2-} \rightarrow Co^{3+}$ and the $^1A_{1g} \rightarrow {}^1T_{2g}$ transition, due to Co(III) in octahedral geometry. The second band, with a maximum observed at 650 nm for the bulk and 569 nm for the Nps, is related to the second $^1A_{1g} \rightarrow {}^1T_{1g}$ transition, assigned to Co(III) in octahedral geometry and the $^4A_2 \rightarrow {}^4T_1$ transition attributable to Co(II) in tetrahedral geometry[42]. For semiconductor materials the quantum confinement effect is expected if the semiconductor size becomes smaller than the Bohr radius of the exciton, and the absorption edge is shifted to a higher energy. In this case, the absorption spectrum of Co_3O_4 Nps shows an absorption edge value at 700 nm (1.76 eV) in comparison with the corresponding Co_3O_4 bulk at 949 nm (1.30 eV). This important blue shift of 249 nm is a clear evidence of the quantum size effect.

Moreover, the Raman spectroscopy is a nondestructive technique which in the last years has been extensively used in nanostructure characterization, the corresponding Co_3O_4 Nps and bulk Raman spectra are shown in figure 3. These spectra clearly exhibit five well-defined peaks at 189, 515, 609, 475 and 679 cm^{-1}, assigned to the Raman-active modes of the Co_3O_4 spinel with T_{2g}, E_g and A_{1g} symmetries, respectively[43,44]. In the Co_3O_4 Nps Raman spectrum, the peaks appear broadened and additionally a little red shift is observed. This behavior has been observed by other authors, and related to size effect[35].

The HR-TEM micrographs corroborate the formation of small nanocrystals with dimensions close to those determined by X-ray diffraction patterns (figure 4). Representative nanocrystallites obtained from sample A are shown in figure 4a. These nanocrystals have dimensions of 3.7nm×3.6nm (the smallest one) and 6.2nm×5nm (the largest one). While figure 4b shows a nanocrystal with dimensions of 11.8nm×7nm; this mi-

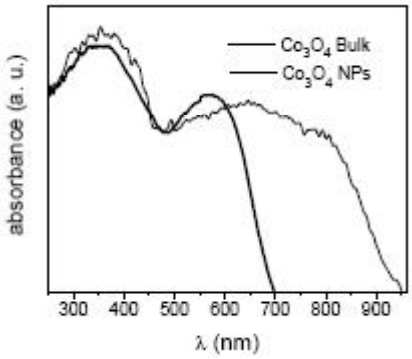

Figure 2: UV-Visible electronic absorption spectra of Co_3O_4 bulk and Nps

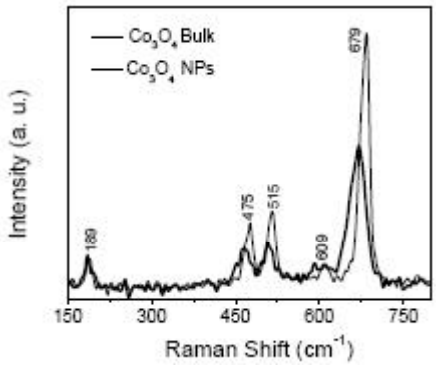

Figure 3: Raman spectra of Co_3O_4 bulk and Co_3O_4 nanoparticles

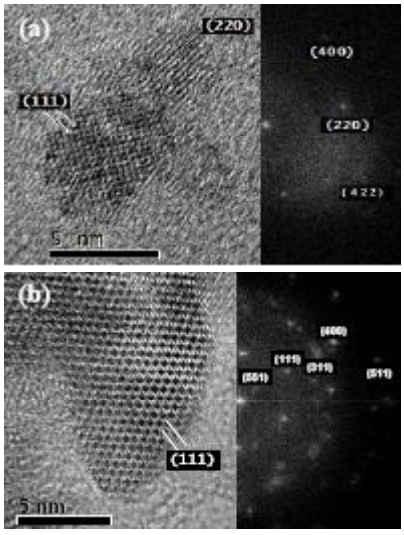

Figure 4: HR-TEM micrographs of Co_3O_4 Nps obtained from (a) sample A and (b) sample B, and their corresponding electron diffraction patterns

crograph was obtained from sample B. The interplanar distances determined from their corresponding electron diffraction patterns confirm that the nanocrystals are composed of Co_3O_4.

On the other hand, CuO Nps were easily obtained at room temperature, after milling in an agate mortar copper salts (chloride or acetate) and sodium hydroxide, about 20 minutes. Their corresponding X-ray diffraction patterns disclose the formation of a nanocrystalline product, all diffraction peaks can be perfectly indexed to the monoclinic CuO tenorite structure (JCPDS card 80-1268). The major peaks located at 2θ values of 20-70° clearly indicate that the CuO product is a pure phase; in addition, the diffraction peaks appear broadened due to fine crystal size(figures 5a and 5b). As a first approximation, crystallite sizes were calculated from Scherrer equation on (-111) and (-202) reflections, finding an average CuO nanocrystal size of 6±0.36 nm when the starting salt was copper acetate (sample C) and 8±0.56 nm when copper chloride was used in the synthesis of CuO Nps (sample D).

The optical response of CuO Nps was evaluated by UV-Visible electronic absorption spectra, obtained by DRS. As shown in figure 6, the spectra of CuO bulk and Nps exhibit broad absorption bands, centered at 582 nm for the bulk and about 356 nm for the Nps. The absorption edge values are observed at 817 nm (1.5 eV) and 633 nm (1.95 eV) respectively. This important blue shift manifests the quantum confinement effect.

To further identify the composition of the copper oxide nanoparticles, Raman spectra were measured at room temperature. CuO presents three typical Raman-active modes with Ag and 2Bg geometries. These characteristic bands appear at 292, 338 and 631 cm^{-1} for the CuO bulk Raman spectrum. In comparison the Raman peaks of the CuO Nps are broadened and shifted to 273, 325 and 607 cm^{-1} due to the size effects of the CuO nanoparticles[35](Figure 7).

Typical HR-TEM micrographs obtained from sample C are shown in figures 8a and 8b. In these micrographs, nanocrystallites with dimensions close to those determined by X-ray diffraction patterns can be observed. While a representative single nanocrystal with dimensions of 3.4 nm×3.8 nm of CuO Nps (sample D) is observed in figure 8c. Also, the electron diffraction

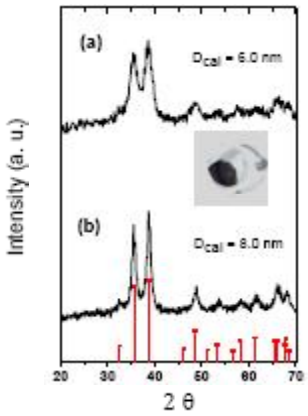

Figure 5: XRD patterns of CuO Nps obtained from (a) copper acetate salt (sample C) and (b) copper chloride salt (sample D)

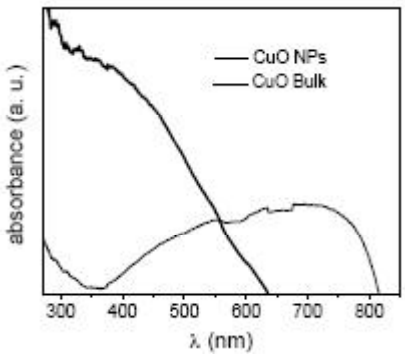

Figure 6: UV-visible electronic absorption spectra of CuO bulk and nanoparticles

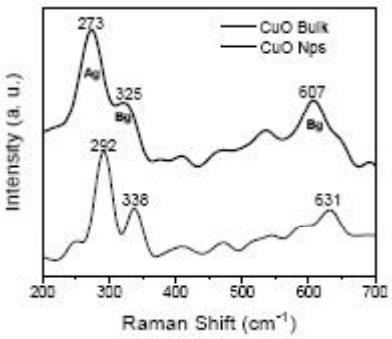

Figure 7: Raman spectra of CuO bulk and nanoparticles

patterns confirm the nanocrystals to be composed of CuO.

A principal effect of finite size is the breaking of a large number of bonds on the surface cations, producing a core of coupling spins, surrounded by a disordered shell. This can result in a disordered spin configuration near the surface and a reduced average net moment compared to the bulk materials. In nanoparticles

Full Paper

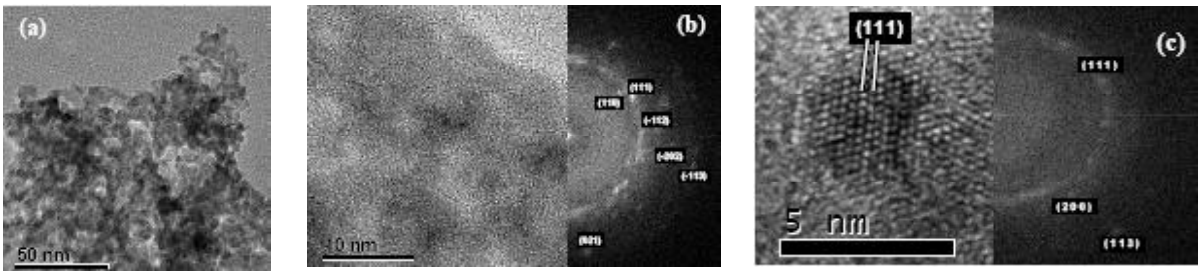

Figure 8: (a) TEM and (b) HR-TEM micrographs of CuO Nps (sample C), and (c) HR-TEM micrograph of CuO Nps (sample D) and their corresponding electron diffraction patterns

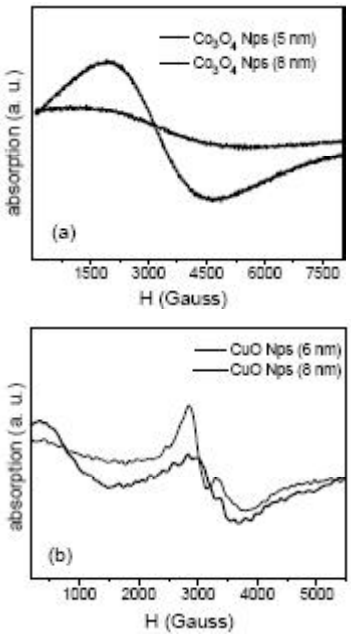

Figure 9: X-band EPR spectra obtained at room temperature of (a) Co_3O_4 Nps and (b) CuO Nps

with an antiferromagnetically ordered core, the surface spins are expected to dominate the measured magnetization due to their lower coordination and uncompensated exchange couplings[34].

In order to study the magnetic response of nano particles, X-band EPR spectra of Co_3O_4 and CuO nanostructures were obtained at room temperature, under the experimental conditions described. In the Co_3O_4 Nps EPR spectra, shown in figure 9a, very broad absorption bands, which are more intensive for the smaller nanoparticles, are observed. This behavior has been ascribed to weak antiferromagnetic coupling. On the other hand, in the EPR spectra of CuO Nps, shown in figure 9b, broad absorption bands of a weak paramagnetic axial signal are observed. In addition, for the smaller one, an absorption band at low magnetic field appears.

As expected, the magnetic behavior is under the influence of nanoparticle size effects as well as intrinsic defects like cation or anion vacancies.

It is probable that in both nanosystems a weak ferrimagnetic coupling happen at low temperatures. Nevertheless, it is necessary to carry out a magnetization experiment and hysteresis loop, in order to confirm this possibility.

CONCLUSIONS

We have demonstrated that a solvent-free mechanochemical solid-solid method can be employed to obtain Co_3O_4 and CuO nanoparticles in mild reaction conditions. This procedure is clean, reproducible, environment friendly and can be extended to other transition metal oxides as Mn_3O_4 and Fe_3O_4. The key to obtain small nanoparticles is the concentration of the starting salts, and in both cases when the acetate is involved in the reaction system, smaller nanoparticles were obtained

ACKNOWLEDGMENTS

The support of this research by the PAPIIT project IN109205 is gratefully acknowledged. We would like to thank Josefina Elizalde-Torres for the technical support.

REFERENCES

[1] A.Punnoose, H.Magnone, M.S.Seehra; Phys.Rev., **B64**, 17420 **(2001)**.

[2] Y.Ichiyanagi, S.Yamada; Polyhedron, **24**, 2813 **(2005)**.

[3] S.A.Makhlouf; J.Magn.Magn.Mater., **246**, 184 **(2002)**.
[4] H.R.Chen, J L.Shi, Y.S.Li, J.N.Yan, Z.L.Hua, H.G. Chen, D.S.Yan; Adv.Mater., **15**, 1708 **(2003)**.
[5] N.Perkas, Y.Koltypin, O.Palchik, A.Gedanken, S. Chadrasekaran; Appl.Catal.A: Gen., **209**,125 **(2001)**.
[6] N.Pinna, G.Neri, M.Antonietti, M.Niederberger; Angew.Chem.Int.Ed., **43**, 4345 **(2004)**.
[7] S.C.Pillai, J.M.Kelly, D.E.McCormack, R.Ramesh; J.Mater.Chem., **14**, 1572 **(2004)**.
[8] W.S.Seo, H.H.Jo, K Lee, B.Kim, S.J.Oh, J.T.Park; Angew.Chem.Int.ed., **43**, 1115 **(2004)**.
[9] J.VanElp, J.L.Wieland, H,Eskes, P.Kuiper, G.A. Sawatzky, F.M.F.de Groot, T.S.Turner; Phys.Rev., **B 44**, 6090 **(1991)**.
[10] C.Mocuta, A.Barbier, G.Renauld, App.Surf.Sci., **56**, 162 **(2002)**.
[11] X.Wang, X.Chen, L.Gao, H.Zheng, Z.Zhang, Y. Qian, J.Phys.Chem., B**108**, 16401 **(2004)**.
[12] 12.M.Sato, S.Kohiki, Y.Hayakawa, Y.Snoda, T. Babasaki, H.Deguchi, M.Mitome, J.Appl.Phys., **88**, 2771 **(2000)**.
[13] M.Andok, T.Kobayashi, S.Lijima, M.J.Haruta, Mater.Chem., **7**, 1179 **(1997)**.
[14] M.M.Natile, A.Glisenti; Chem.Mater., **14**, 3090 **(2002)**.
[15] T.Maruyama, S.J.Arai; Electrochem.Soc., **143**, 1383 **(1996)**.
[16] G.XWang, Y.Chen, K.Konstantinov, J.Yao, J.H.Ahn, H.K.Lui, S.X.Dou; J.Alloys.Compd., **340**, 5 **(2002)**.
[17] J.Liu, X.Huang, Y.Li, K.M.Sulieman, X.He, F.Sun; Crystal Growth and Desing, **6**, 1690 **(2006)**.
[18] H.Fan, L.Yang, W.Hua, X.Wu, Z.Wu, S.Xie, B.Zou; Nanotechnology, **15**, 37 **(2004)**.
[19] K.Muraleedharan, C.K.Subramaniam, N. Venkataramani, T.K.Gundu Rao, C.M.Srivastava, V.Sankaranarayan, R.Srinivasan; Solid State Commun., **76**, 727 **(1990)**.
[20] J.Hwang, T.Timusk, G.D.Gu; Nature, **427**, 714 **(2004)**.
[21] H.Takeda, K.Yoshino; Phys.Rev., **B67**, 5109 **(2003)**.
[22] M.Frietsch, F.Zudock, J.Goschnick, M.Bruns; Sens.Actuators, **B 65**, 379 **(2000)**.
[23] X.G.Wen, Y.T.Xie, C.L.Choi, K.C.Wan, X.Y.Li, S.H.Yang; Langmuir, **21**, 4729 **(2005)**.
[24] X.P.Gao, J.L.Bao, G.L.Pan, H.Y.Zhu, P.X.Huang, F.Wu, D.Y.Song; J.Phys.Chem., **B108**, 5547 **(2004)**.
[25] R.Tongpool, C.Leach; J.Mater.Sci.Lett., **19**, 119 **(2000)**.
[26] L.Zhou, J.Xu, X.Li, F.Wang; Mater.Chem.Phys., **97**, 137 **(2006)**.
[27] R.Yang, L.Gao; Chem.Lett., **33**, 1194 **(2004)**.
[28] Y.Chang, H.Ch.Zeng; Crystal Growth and Desing, **4**, 397 **(2004)**.
[29] H.Wang, J.Z.Xu, J.J.Zhu, H.Y.Chen; J.Cryst. Growth, **244**, 88 **(2002)**.
[30] Z.Yang, J.Xu, W.Zhang, A.Liu, S.Tang; J.Solid State Chem., **180**, 1390 **(2007)**.
[31] W.Wang, Y.Zhan, X.Wang, Y.Liu, Ch.Zheng, G.Wang; Mater.Res.Bulletin, **37**, 1093 **(2002)**.
[32] A.L.Fernandez-Osorio, A.Vazquez-Olmos, E.Mata-Zamora, J.M.Saniger; J.Sol-Gel.Sci.Techn., **42**, 145 **(2007)**.
[33] A.Vazquez-Olmos, R.Redon, M.E.Mata-Zamora, F.Morales-Leal, A.L.Fernandez-Osorio, J.M. Saniger; Rev.Adv.Mater.Sci., **10**, 362 **(2005)**.
[34] A.Vazquez-Olmos, R.Redon, G.Rodriguez-Gattorno, M.E.Mata-Zamora, F.Morales-Leal, A.L. Fernandez -Osorio, J.M.Saniger; J.Colloid Interf. Sci., **291**, 175 **(2005)**.
[35] J.F.Xu, W.Ji, Z.X.Shen, S.H.Tang; J.Solid State Chem., **147**, 516 **(1999)**.
[36] G.García-Pacheco, J.G.Cabanas-Moreno, H.Yee-Madeira, F.Cruz-Gandarilla; Nanotech., **40**, 1929 **(2005)**.
[37] V.Sepelak, I.Bergmann, S.Kiip, K.D.Becker; Z.Anorg.Allg.Chem., **631**, 993 **(2005)**.
[38] V.V.Boldyrev; Russian Chem.Revs., **75**, 177 **(2006)**.
[39] A.L.Garay, A.Pichon, S.L.James; Chem.Soc.Rev., **36**, 846 **(2007)**.
[40] L.Frazer; Environmental Health Perspectives, **111**, A534 **(2003)**.
[41] A.Alacova, J.Ficeriova, M.Golja; Metalurgijca, **43**, 305 **(2004)**.
[42] L.G.A.van de Water, G.L.Bezemer, J.A.Bergwerff, M.Versluijs-Helder, B.M.Weckhuysen, K.P.de Jong; J.Catal., **242**, 287 **(2006)**.
[43] D.Gallant, M.Pézolet, S.Simard; J.Phys.Chem., **B110**, 6871 **(2006)**.
[44] R.Sato-Berru, A.Vazquez-Olmos, A.L.Fernandez-Osorio, S.Sotres-Martinez; J.Raman.Spectrosc., **38**, 1073 **(2007)**.